3E04

On the environmental stability of methylammonium lead/tin halide ($CH_3NH_3Pb(/Sn)X_3$) perovskites

(Department of Chemical System Engineering, School of Engineering, The University of Tokyo, 7-3-1 Hongo, Bunkyo-ku, Japan 113-8656)

[O] Arpita Varadwaj, Pradeep R. Varadwaj, Koichi Yamashita

E-mail: arpita@tcl.t.u-tokyo.ac.jp

[Introduction] Scientists categorize methylammonium lead(/tin) trihalides as possible potential candidates for the third-generation of photovoltaic solar cells.[1] They are represented by the chemical formula $CH_3NH_3Pb(/Sn)X_3$ (X = Cl, Br, I). They are soft nanomaterials, which are a class of hybrid minerals formed of an unusual mixing of two different ionic species, the $CH_3NH_3^+$ organic cation and the $[Pb(/Sn/Ge)X_3]^-$ inorganic anion, which are the key ingredients for the building block. The above formula belongs to the ABX_3 perovskite family; the most common one in this family is discovered to be $CaTiO_3$. Clearly, the formulations above possess structural similarities that explain why the mixtures comprising the lead or tin trihalides and the methylammonium are referred to as organic-inorganic hybrid perovskites. Notable is their extraordinary mechanical and technological breakthroughs for which they have gone viral in academics, as well as in the solar sector today.[2] For instance, the halide perovskites display large optical (photo) absorption coefficients > 16 mm^{-1}.[2] They carry giant static dielectric constants ranging between 60 and 70, low exciton binding energies approximately close to 16 meV at low temperatures, exceptional minority carrier lifetimes close to 280 ns, long electron and hole diffusion lengths up to 175 microns, high charge carrier mobilities < ~100 $cm^2/(Vs)$, and very low effective masses of electrons and holes (viz. tetragonal: 0.197 vs. 0.340 m_0; orthorhombic: 0.239 vs. 0.357 m_0), excellent for transport.[3]

An attribute exposing the halide perovskites to scientific communities is photovoltaic conversion efficiency (PCE). (The term *efficiency* refers a fraction of sunlight energy converted to the electrical energy *via* the photovoltaic technology.) The National Renewable Energy Laboratory (NREL) certified PCE ranges up to 22.1%, reported early this year.[4] This is indeed a fantastic improvement compared not only to the prior value of 3.8% reported for the first time in 2009,[5] but also to the crystalline silicon solar cells that have taken decades to reach a PCE somewhat closer to the above value. It is recently showed that when the mixed cesium cation lead mixed-halide perovskite tendem solar cells combine with the 19%-efficient silicon solar cell, it would result in the feasibility of achieving an efficiency of conversion even greater than 25%.[5] Nevertheless, an obvious feature that lifts the perovskite materials to a top level lies in a measurable property called optical band gap energy. It is tunable in the 1.5 to 3.1 eV range, with a value of < 1.6 eV being recommended for device performance. The featured characteristics mentioned above, together with their excellent transport properties, might explain why the halide perovskites do have propitious potentials to serve as p–i–n type semiconductor junction (photo)diodes. Nonetheless, many researches are currently ongoing in this filed to identify factors influencing the chemico-technological improvement of the PCE, the origins of anomalous hysteresis in the current–voltage characteristics, and the origins of the ferroelectricity, etc., observed for the highest efficient lead iodide perovskite. In contrary, several other researchers are involved to explore factors responsible explaining the observed air and moisture instabilities of the $CH_3NH_3Pb(/Sn)X_3$ perovskite films. Whilst a number of experimental observations on the latter topic have led to diverse views, there is almost no theoretical attempt placed to insight into the chemical physics of the anhydrate perovskites in water (H_2O). Herein, we report the electronic structure, binding energy, molecular band gap, and electron density topological property results of several hydrated clusters of the $[Pb/SnI_6(MA)_8]^{4+}$ cation in zero-dimension, where MA refers to $CH_3NH_3^+$. These results are achieved combining Density Functional Theory (DFT) with Quantum Theory of Atoms in Molecules (QTAIM) calculations. Finally, the results are compared with those already reported for the $MAPb(/Sn)X_3$ perovskites in higher dimensions. The study has boosted us concluding whether or not the environmental species, e.g. H_2O, is fully responsible for degrading the halide perovskites.

[Results and discussions] Two conflicting views are advised in the literature in connection with the environmental stabilities of the halide perovskites. According to a bunch of authors, including Mitzi and colleagues,[6b] Kamat and coworkers,[6a] and others,[6c)–e)] the halide perovskites are not air, moisture, and humidity stable because they are highly sensitive to the environment. According to Frost et al., [6d] a single water molecule is sufficient to degrade the halide perovskites when it comes into contact with, but an excess of it would dissolve the HI and CH_3NH_2 byproducts, as well as to degrade the material completely to form PbI_2. Perhaps this suggestion is consistent with those of Kamat et al. and others.[6a] For instance, these latter authors have suggested that the possible reaction pathway for the decomposition of the $CH_3NH_3PbI_3$ perovskite in the presence of H_2O is: $CH_3NH_3PbI_3$ (solid) ⟶ CH_3NH_2 (gas) + HI (gas) + PbI_2 (solid). The $CH_3NH_3PbI_3$ species upon its exposure to moisture forms mono- and di-hydrates, $CH_3NH_3PbI_3{\bullet}H_2O$ and $(CH_3NH_3)_4PbI_6{\bullet}H_2O$, respectively, as the integral parts of the degradation mechanism. And that the introduction of the H_2O molecule into the geometry of the lead iodide perovskite not only result in the widening of the band gap of the material, but also changes its surface morphology.

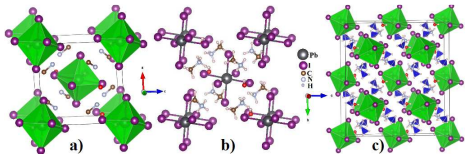

Fig.1. The a) polyhedral, and b) ball and stick models for the packing of the $(CH_3NH_3)_4PbI_6{\bullet}2H_2O$ crystal as of the Cambridge Structure Database (CSD) (ref. code FOLLIB). Shown in c) is a 1x2x3 slab model of the aforesaid crystal reported by Wakamiya et al. (CSD ref. code, FOLLIB01). For clarity, H atoms are omitted in a).

Oppositely, a recent experimental investigation of Manshor et al. demands that the $CH_3NH_3PbI_3$ film is only *a little* affected upon its exposure to humidity.[7a] Its major degradation occurs when it is exposed with photon dose. This conclusion was drawn after the $MAPbI_3$ pristine films were exposed separately to both dark and light. It made the film to result in more intense degradation despite their ~7 times shorter shelf-life (~ 100 h) in light relative to that observed in the dark (~ 600 h). Contrariwise, when the authors exposed the $CH_3NH_3PbI_3$ PeP films to humidity in dark, they did not observe the presence of the PbI_2, suggesting the film was not degraded. However, the authors did observe a change in the color of the film from dark to light brown, which they recognized as a consequence of structural variations in the film. Note that when the 5, 10, and 20 wt% films of the latter type were placed in light, they underwent significant degradation especially in the interface region formed between the TiO_2 electron transport layer and the perovskite films, consistent with observations of others.[7b)–c)] These were contradictory with those the pristine films exposed to similar environments, which resulted in complete degradation of the films leading to PbI_2. Consequently, these results propagandize the degradation of both the film types mainly by photon dose under humid condition.

Nevertheless, there are about three crystallographic structures reported for hydrated $CH_3NH_3PbI_3$, catalogued in the Cambridge Structural Database (CSD). These include one $CH_3NH_3PbI_3{\bullet}H_2O$[8a] and two $(CH_3NH_3)_4PbI_6{\bullet}2H_2O$.[8b)–c)] The former and latter structures reported in 1987 and 2014 are having P21/n and P21/m space group symmetries, respectively. Figs. 1 a) & c) display the packed polyhedral, and b) the ball & stick models of the $(CH_3NH_3)_4PbI_6{\bullet}2H_2O$ crystal reported in 1987,[8b)] consisting of a distorted fcc array of the PbI_6^{4-} ions interspersed with the $CH_3NH_3^+$ cations of two types and H_2O molecules of a single type. Fig. 1 c) shows a 1x2x3 slab model for the hydrated structure reported by Wakamiya and coworkers,[8c)] displaying the structural evolution of the unit cell, which has identical stoichiometry relative to the crystal reported in 1987,[8b)] and that the H_2O molecules in this crystal were introduced by exposing the sample to air. Nevertheless, as displayed in Fig. 1, both the crystals contain several PbI_6^{4-} octahedra in higher dimension in which the each of the eight faces of a given octahedron can be realized

equipped with an MA species, that is, $[PbI_6(MA)_8]^{4+}$. The attribute is not only reminiscent of the crystal of $CH_3NH_3PbI_3$ in the monoclinic phase, but also evident of its other known phases (viz. see *abstract 3E03* for the pseudocubic phase).

While many possibilities exist, five conformers for each of the $[Pb(/Sn)X_6(MA)_8]^{4+}$ cations were optimized with DFT-PBE/DZP, see Fig. 3a). The most stable of these in each set is found to be a structure with center of inversion symmetry, C_i, $[Pb(/Sn)I_6(MA)_8]^{4+}$. The physical orientations of the $CH_3NH_3^+$ cations around the first coordination sphere of the $[PbX_6]^{4-}$ anion in this stable cluster are similar to that of the $(CH_3NH_3)_4^{4+}\bullet[PbI_6]^{4-}\bullet(H_2O)_2$ crystal, CSD ref. code FOLLIB. Its geometry is about 5.5, 24.7, 24.8, and 103.8 kcal mol^{-1} relatively more stable than the four other high energy conformers identified (Fig. 3a)). Of these latter four, the geometries of the intermediate two are first and second order saddle points, and the other two are genuine local minima. In all the high energy clusters, the eight organic cations facing the centers of the eight faces of the $[PbX_6]^{4-}$ octahedron are perhaps significantly hydrogen bonded.

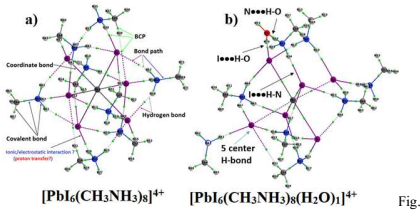

$[PbI_6(CH_3NH_3)_8]^{4+}$ $[PbI_6(CH_3NH_3)_8(H_2O)_1]^{4+}$ Fig. 2: Examples of QTAIM molecular graphs of the anhydrate (a) and hydrated (with one H_2O molecule) clusters of the $[PbI_6(CH_3NH_3)_8]^{4+}$ cation, unraveling weak-to-strong interactions.

As already noted, the main focus of this investigation was to theoretically assess how, and to what extent, the $[PbI_6(MA)_8]^{4+}$ coordination sphere can be affected by adding ten H_2O molecules around its surrounding, one at a time systematically in a stepwise manner. Since the DFT-PBE/DZP method (relative to many other DFT functionals and basis sets) produces the molecular HOMO-LUMO gap energy for the zero-dimensional $CH_3NH_3PbI_3$ cluster somehow closer to experimental band gaps reported for the higher dimensional analogues, the same method was utilized for the energy-minimization of the $[Pb(/Sn)X_6(MA)_8]^{4+}$ (X = Cl, Br, I) octahedra. Later, the H_2O molecules were added one by one to the outer second coordination spheres of each of the $[Pb(/Sn)X_6(MA)_8]^{4+}$ systems in a stepwise manner. The process was continued until all the $[(Pb(/Sn)I_6(MA)_8)\bullet\bullet\bullet(H_2O)_{n=1-10}]^{4+}$ cationic clusters were fully energy minimized.

While the knowledge of the positions of the H atoms in MA in the $(CH_3NH_3)_4PbI_6\bullet 2H_2O$ crystal is completely lacking, the nature of hydrogen bonding interactions discussed in the literature is purely arbitrary.[8b)] Fig. 2 depicts QTAIM molecular graphs for two selected clusters, the anhydrate $[PbI_6(MA)_8]^{4+}$ and the (single water) hydrated $[PbI_6(MA)_8(H_2O)_1]^{4+}$. It has greatly assisted us in identifying various kinds of such interactions, consistent with the recommended IUPAC signatures. For instance, the anhydrate cluster is stabilized by means of an extensive network of I•••H–N(MA) and I•••H–C(MA) intermolecular hydrogen bonded interactions, in which each MA involves in three of them. Such identifications are relied on the presence of the bond critical points (BCPs) of charge density between atomic basins, and the bond paths that connect them, and the short-to-long intermolecular distances for the above interactions (2.427–2.660 vs. 2.832–3.530 Å). The short I•••H–N distances explain the $–NH_3$ part of MA is prone to reaction as is always observed tilted towards the face center, or the corner, or the edge of the octahedron in majorities of the halide perovskites crystals catalogued.

Upon an addition of a single H_2O molecule to the second coordination sphere of the $[PbI_6(MA)_8]^{4+}$ ion, the geometry of the ion in the modified species is distorted, but it is not very significant that can degrade the close-shell system completely, as suggested.[6d)] As in Fig. 2b, a single H_2O molecule upon its introduction has displayed its sufficient potential to leak into the second coordination shell formed of the MA ions. A consequence of this is that the highly competitive hydrogen bonding interactions between I and H_2O, MA and H_2O, and I and MA experience significant push-ups due to steric reasons, leading the MA ions (compared to the H_2O) to move further away. The result explains why some of the MAs in Fig. 2 govern singular hydrogen bonding interactions with the I atoms in $[(CH_3NH_3)_8^{8+}\bullet[PbI_6]^{4-}\bullet(H_2O)_1]$.

The I atoms in $[PbI_6]^{4-}$ serve as four- and/or five-center hydrogen bond acceptors in presence of H_2O, an unified feature that has never enlightened before. Since the H_2O species is smaller than MA and has an adamant of forming hydrogen bonding interactions, it forms two such interactions with its two proton donors upon its interaction with the I atoms in $[(CH_3NH_3)_8[PbI_6]^{4+}$. In the meantime, as an acceptor of hydrogen bonds, the O atom of it simultaneously involves in predominant proton transfer reactions with the protons of the $–NH_3$ fragment in MA. Because of this latter feature, and because of the presence of unavoidable steric crowding between the H_2O and MA species in the second coordination sphere, the latter species will be pushed backward. This situation is displayed in Fig. 2 (right). Note that the addition of more H_2O molecules to the second coordination sphere of the $[(PbI_6(MA)_8)]^{4+}$ ion results in the facilitation of significant proton transfer reactions between the H_2O molecules and the MA species in the modified clusters. At this stage, if the perovskite material is exposed with significant photon dose, or with high temperatures, it would probably undergo significant structural decomposition. Through this way, there are significant chances for the sublimation of various species, e.g., NH_3CH_3I, CH_3NH_2 and HI, etc., leaving the PbI_2 solid species alone.

A single H_2O molecule on the outer sphere of the $[(PbI_6(MA)_8)]^{4+}$ cation produces an uncorrected binding energy ΔE of –40.2 kcal mol^{-1}. Successive increase in the number of H_2O molecules around the cation increases the ΔE values for the hydrated cluster ions. The trend in increase in ΔE is non-additive cooperative. The most stable cation has ten H_2O molecules, $[(PbI_6(MA)_8)\bullet\bullet\bullet(H_2O)_{10}]^{4+}$, with $\Delta E \sim –291.0$ kcal mol^{-1} (roughly –29.1 kcal mol^{-1} per H_2O). Fig. 3 shows a linear relationship between the number of the H_2O molecules n in the $[(Pb(/Sn)X_6(MA)_8)\bullet\bullet\bullet(H_2O)_{n=1-10}]^{4+}$ ion and the ΔE. The graphs indicate that although the H_2O molecules distort the geometries of the $[(Pb(/Sn)X_6(MA)_8)]^{4+}$ ions, they increase the overall stabilities of the hydrated clusters at 0 or 298.15 K. At this range of temperatures, the perovskites might not degrade completely. The conclusion is also decisive regardless of the dimensionality of the halide perovskites.

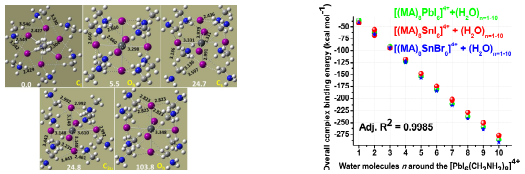

Fig. 3 a) The conformers of the $[PbI_6(MA)_8]^{4+}$ ion & b) the linear dependence of overall binding energy on the number of H_2O molecules n for the $[[PbI_6(CH_3NH_3)_8]\bullet\bullet\bullet(H_2O)_{n=1-10}]^{4+}$ clusters. The data points are fitted to a linear equation of the form: $\Delta E = a\times n + b$.

The HOMO-LUMO gap is an important measure of the device quality of a material. Its value for $[(PbI_6(MA)_8)]^{4+}$ is PBE/DZP calculated to be 3.07 eV. Addition of two H_2O molecules (first and second) around the coordination sphere of the ion has downshifted the gap to 2.65, and 2.62 eV, respectively. However, increasing this number to three (or, even up to ten) around the $[(PbI_6(MA)_8)]^{4+}$ ion, the gap further increases in which the gap oscillates between 3.05 and 3.25 eV for all the cationic clusters investigated. For instance, the value of this gap was ca. 3.09, 3.13, 3.25 and 3.24 eV for $[(PbI_6(MA)_8)\bullet\bullet\bullet(H_2O)_3]^{4+}$, $[(PbI_6(MA)_8)\bullet\bullet\bullet(H_2O)_4]^{4+}$, $[(PbI_6(MA)_8)\bullet\bullet\bullet(H_2O)_6]^{4+}$ and $[(PbI_6(MA)_8)\bullet\bullet\bullet(H_2O)_{10}]^{4+}$, respectively. This may mean the optical gap is almost unaffected by the presence of the H_2O molecules despite the significant geometrical distortions encountered. The conclusions drawn above for the $[PbI_6(MA)_8]^{4+}$ hydrated systems can be applicable to the other hydrated clusters, viz. $[PbX_6(MA)_8]^{4+}$ (X = Cl, Br) and $[SnX_6(MA)_8]^{4+}$ (X = Cl, Br, I).

[References]

[1] a) J. Yan, B. R. Sounders, RSC Adv. 2014, 4, 43286; b) T. C. Sum et al., Acc. Chem. Res. 2016, 49, 294.

[2] T. -B. Song et al., J. Mater. Chem. A 2015, 3, 9032.

[3] a) Miyata et al, Nat. Phys. 2015, 11, 582; b) R. E. Brandt, V. Stevanović, D. S. Ginley, T. Buonassisi, MRS Commun. 2015, 5, 265; c) T. M. Brenner, D. A. Egger, A. M. Rappe, L. Kronik, G. Hodes, D. Cahen, J. Phys. Chem. Lett. 2015, 6, 4754.

[4] See the photovoltaic solar cell chart at: http://www.nrel.gov/ncpv/images/efficiency_chart.jpg

[5] a) McMeenkin et al., Science 2016, 351, 151; b) S. Yakunin et al., Nat. Photonics 2015, 9, 444.

[6] a) J. S. Manser et al., Acc. Chem. Res. 2016, 49, 330; b) B. Saparov et al., Chem. Rev. 2016, 116, 4458; c) D. Li et al., J. Phys. Chem. C 2016, 120, 6363; d) J. M. Frost, Nano Lett. 2014, 14, 2584; e) T. A. Berhe et al., Energy Envirno. Sci. 2016, 9, 323.

[7] a) N. A. Manshor et al., Phys. Chem. Chem. Phys.2016, DOI: 10.1039/C6CP03600G; b) F. Matsumoto, J. Phys. Chem. C 2015, 119, 20810; c) J. Xiong et al., Org. Electron. 2016, 30, 30.

[8] a) F. Hao et al., J. Am. Chem. Soc. 2014, 136, 16411; b) B. R. Vincent et al., Can J. Chem. 1987, 65, 1042; c) A. Wakamiya et. al., Chem. Lett. 2014, 43, 711.